Eur. Radiol. 6, 473–480 (1996)

Ultrasound

European Radiology

Original article

Vascular patterns in reactive and malignant lymphadenopathy

A. Tschammler[1], H. Wirkner[1], G. Ott[2], D. Hahn[1]

[1] Institut für Roentgendiagnostik der Universität Würzburg, Josef-Schneider-Strasse 2/Bau 4, D-97080 Würzburg, Germany
[2] Pathologisches Institut der Universität Würzburg, Josef-Schneider-Strasse 2 D-97080 Würzburg, Germany

Received 16 February 1995; Revision received 24 August 1995; Accepted 13 September 1995

Abstract. A total of 130 superficial lymph nodes were evaluated using color Doppler flow imaging (CDFI) in order to differentiate benign from malignant lymphadenopathy. The patterns of intranodal flow signals detected at standardized conditions by CDFI were classified using eight self-defined criteria and were correlated with the histopathological or clinical diagnosis. Nonparametric discriminant analysis showed that four vascular patterns were suspicious of malignancy: (a) avascular areas, (b) displacement of intranodal vessels, (c) accessory peripheral vessels and (d) aberrant course of central vessels. Of the neoplastic lymph nodes ($n = 73$), 96% showed at least one pathological vascular pattern. Malignancy could be excluded in 95% of 57 reactive lymph nodes using these four criteria. Most reactive lymph nodes in contrast demonstrated a vascular hilus and/or vessels running at the long axis of the lymph node with branches to the cortex. There was a diagnostic accuracy of 41–82% in the additionally evaluated sonomorphological (size, shape, echogenicity) and Doppler (increased Pourcelot's or pulsatility indices) criteria. The definitive interpretation of the promising results of this retrospective study requires confirmation of examiner independency as well as a prospective evaluation.

Key words: Color Doppler flow imaging – Ultrasonography – Lymphoma – Lymph node – Lymph node blood supply

Introduction

Ultrasonography is a highly sensitive method to detect pathological lymph node alterations. Changes in the size [1, 2], shape [3] and echogenicity [4, 5] were assessed in order to differentiate benign from malignant lymphadenopathy. However, up to the present none of these criteria have attained a sufficient diagnostic accuracy. Color Doppler flow imaging (CDFI) extended the sonographical diagnostics by the assessment of the vascularity of superficial lymph nodes and by the Doppler spectral analysis of intranodal vessels [6, 7]. Microangiographic and pathophysiological studies [8, 9] observed hypervascularity and a direct correlation between perfusion and volume in acute lymphadenitis. In malignant lymphadenopathy necroses or arteriovenous shunts may lead to quantitative and qualitative changes in the perfusion. Alterations in the vascular pattern in lymph node metastases were reported in singular angiographic studies [10, 11]. The current study classified the patterns of the intranodal vascularization and sonomorphological changes which were detected by CDFI in reactive lymph nodes and in lymph nodes which were infiltrated by metastases or malignant lymphomas (hereafter referred to as malignant lymph nodes). The results were correlated with the histopathological or clinical diagnosis.

Methods

In 70 patients (51 males and 19 females; age 16–89 years) 130 CDFI studies (QAD1 Philips/Quantum) which were archived digitally on video tapes were reviewed retrospectively by a radiologist who was unaware of the diagnosis. Bias caused by sonomorphological changes could not be eliminated. Only lymph nodes which met the following criteria were evaluated: (a) documentation of the whole lymph node on two planes using a 7.5 MHz linear transducer with a mounted wedge-shaped interface in the low-flow modus; (b) identification of intranodal blood flow by Doppler spectral analysis on two planes; (c) standardized settings of the ultrasound (US) device (power > –6 dB, threshold > 13). Intravascular color saturation could not be assessed in the tiny intranodal vessels, which is why initial color artifacts in the tissue adjacent to the lymph nodes

Correspondence to: A. Tschammler

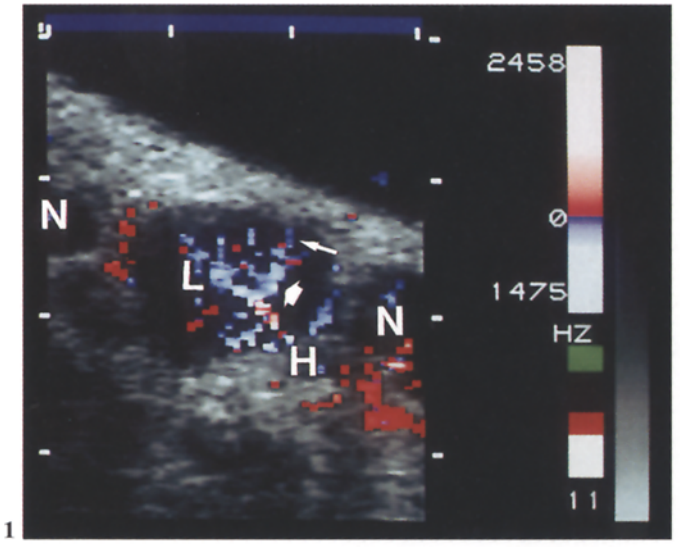

1

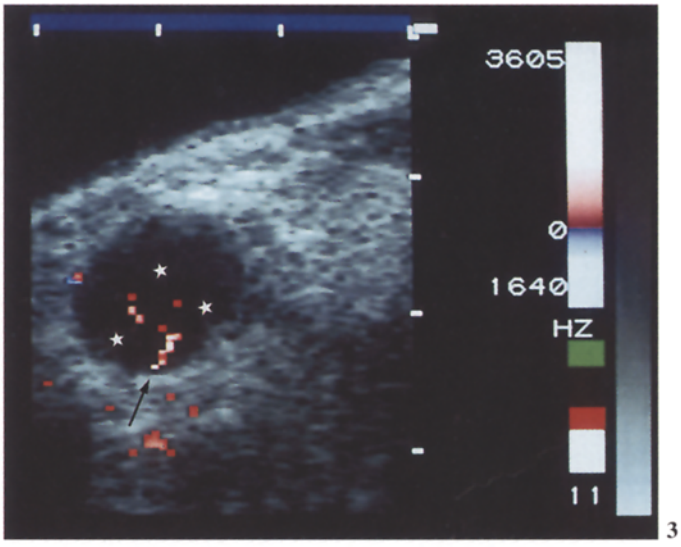

3

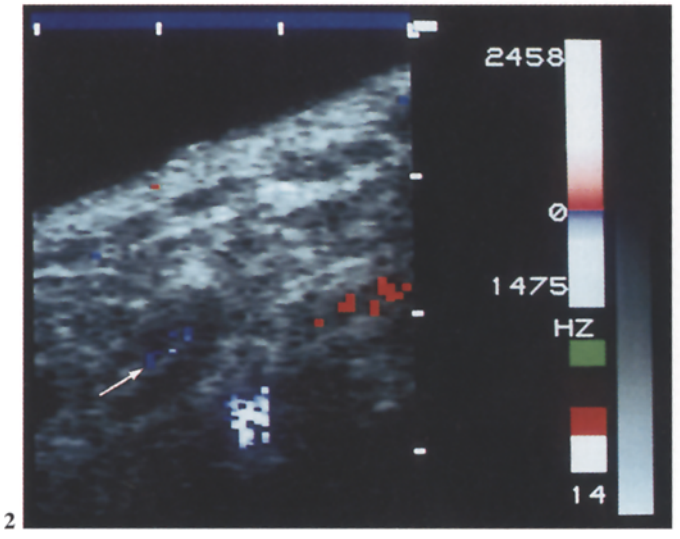

2

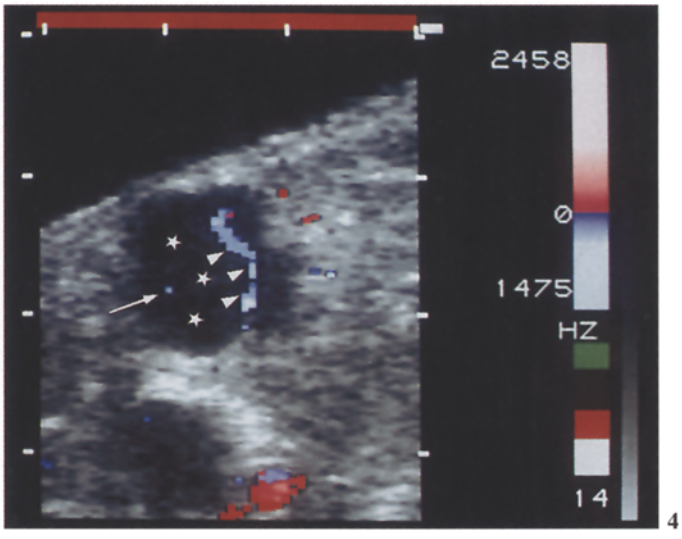

4

Fig 1. Submandibular lymph node (14 × 12 mm) showing a hilar vessel *(H)*, a longitudinal vessel *(L)*, branches of second (◗) and third (→) order, a round shape, and a missing echoic center. Red and blue pixels along the course of the vessels represent adjacent arterial and venous flow signals (proven by Doppler spectral analysis). N = further adjacent submandibular lymph nodes. Diagnosis: acute lymphadenitis, complete regression after antibiotic therapy

Fig. 2. Cervical lymph node (11 × 4 mm) showing flow signals (→) along the long axis (longitudinal vessel without branches). The hilar vessels are not depicted. Sonomorphology: ellipsoid shape, echoic center, narrow hypoechoic rim. Histopathology: unspecific lymphadenitis in a patient showing a carcinoma of the oropharynx

Fig. 3. Submandibular lymph node (10 × 11 mm) showing an aberrant central vessel (→ angle of > 30° with the skin surface), avascular areas *(asterisk)*, a round shape, and a missing echoic center. Histopathology: centroblastic non-Hodgkin's lymphoma

Fig. 4. Cervical lymph node (12 × 11 mm) showing a displacement of an aberrant central vessel (▶), avascular areas *(asterisk)*, and a short vessel segment (→). Sonomorphology: round shape, missing echoic center. Histopathology: lymph node metastasis of a malignant melanoma

were defined as criterion of a individually optimized sensitivity for flow signals. Blood flow which did not induce a Doppler frequency shift of at least 37.5 Hz could not be detected due to a high-pass filter which was set to the lowest cutoff frequency. No lymph nodes were excluded because of impaired image quality.

In contrast to the diagnostics of peripheral vessels, CDFI can frequently only demonstrate short segments of solitary or multiple intranodal vessels in one scan. But careful real-time examination of a whole lymph node on two planes allows the physician to get a virtual image of the three-dimensional (3D) pattern of intranodal flow signals. Eight morphological criteria were defined to classify the patterns of intranodal vascularization which were found by CDFI

1. Detection of an artery and/or a vein crossing the outline of the lymph node at one of the poles of the long axis or at the deepest point (hilar vessels; Fig. 1). If there was only a single color spot at one of these locations on the border of the lymph node it was regarded as a hilar vessel if Doppler spectral analysis showed venous or arterial waveforms, and if it was beyond doubt

that the flow signals were originating from intranodal vessels.
2. Detection of a major artery and/or vein running at the long axis of the lymph node and forming an angle of $\leq 30°$ with the skin surface (longitudinal vessels; Figs. 1 and 2).
3. Detection of vascular branches in the cortex of a lymph node originating symmetrically from the longitudinal vessel (Fig. 1), which was defined as the branch of first order. In malignant lymph nodes the major central vessel was defined as the branch of first order.
4. Scattered or solitary intranodal color signals representing short vessel segments (Fig. 4).
5. One or more major vessels in the center of the lymph node forming an angle of $> 30°$ with the skin surface (aberrant central vessels; Fig. 3).
6. Displacement of intranodal vessels (Fig. 4).
7. Avascular lymph node segments (Fig. 5): focal missing flow signals disproportionate to the vascularization of the remaining lymph node.
8. Vessels in the periphery of a lymph node which do not communicate with hilar or central vessels (accessory vessels; Fig. 6).

Pourcelot's ratio (RI) and the pulsatility index (PI) were calculated in order to quantify pathological ($RI \geq 0.9$; $PI \geq 1.8$) arterial Doppler spectra [6, 7]. The diameters (≤ 10 mm, ≤ 15 mm, > 15 mm) of the lymph node were evaluated on three axes. The shape of the lymph nodes (ellipsoid, round) was assessed according to the ratio between the maximum and minimum diameter (limit maximum/minimum = 2) [3]. The echoic center and hypoechoic rim of the lymph nodes were evaluated in accordance with the criteria published by Vasallo et al. [5]. A score which combined three sonomorphological criteria (Table 1) was calculated. The diagnostic value of these multiple criteria was judged using nonparametric discriminant analysis.

The diagnosis (Table 2) was confirmed by histopathology in 94 lymph nodes. To ensure that examined and removed lymph nodes were identical reports of surgery and histopathology were compared carefully regarding the location and the size reported by sonography. Benign lymph node alterations were diagnosed clinically if regression occurred under antibiotic therapy ($n = 13$) or if there were no signs of malignancy during follow-ups ($n = 23$) of at least 6 months (average 18 months). In order to evaluate the diagnostic value of the pattern of intranodal vessels for the differentiation of benign from malignant lymphadenopathy, a broad spectrum of lymph nodes infiltrated by neoplastic diseases was included in the study. The results of these different entities are presented separately.

Table 1. Sonomorphological index (proposed by P. Vasallo, unpublished) A total of points > 1 indicates malignancy. The hypoechoic rim is not assessed in case of homogeneous hypoechoic lymph nodes

Points	0	1	2
Shape	Ellipsoid	Round	
Echoic center	Normal	Narrow	Missing
Hypoechoic rim	Narrow	Wide	Eccentric

Table 2. Diagnoses of 130 lymph nodes in 70 patients (1–4 lymph nodes/patient)

	N
Benign lymphadenopathy ($n = 57$)	
Mononucleosis	5
Ulcus molle	10
Lues	3
Unspecific	39
Lymph node metastases ($n = 37$)	
Squamous cell carcinoma (all head and neck tumors)	23
Breast cancer	4
Malignant melanoma	9
Cylindroma	1
Malignant lymphomas ($n = 36$)	
Low-grade non-Hodgkin's lymphoma	13
High-grade non-Hodgkin's lymphoma	18
Hodgkin's lymphoma	5

Table 3. Normal patterns of intranodal vascularization detected by color Doppler flow imaging (CDFI) in 130 lymph nodes

	Reactive ($n = 57$)	Metastasis ($n = 37$)	Malignant lymphoma ($n = 36$)
Normal vascular patterns			
Hilar vessels	47	20	27
Longitudinal vessels***	36	4	6
Branching of the longitudinal vessels	25	0	2
Vessel segments	5	5	2
Pathological vascular patterns			
Avascular areas***	2	30	24
Aberrant vessels***	2	15	27
Displacement***	2	21	17
Accessorial vessels***	2	27	18

*** $p < 0.001$

Results

Quality was judged to be good in 107 of the 130 sonographical studies; the rest ($n = 23$) were impaired by artifacts. The quality of 81 Doppler spectra was good; 31 spectra showed artifacts and 23 spectra could not be evaluated quantitatively. A total of 51 lymph nodes showed low vascularization (lower or equal vascularization compared subjectively to those of the adjacent tissue), and 79 lymph nodes were hypervascularized. Branches of second order were found on an average in hypervascularized lymph nodes. Hypovascularized lymph nodes showed branches of first order or short intranodal vessel segments.

Color Doppler flow imaging depicted hilar vessels in 47 (82 %) and/or longitudinal vessels in 36 (63 %) reactive lymph nodes (Table 3). If the hilar vessels entered the lymph node at its deepest point, the longitudinal vessels were spreading symmetrically toward both poles of the long axis. Frequently, a parallel course of adjacent

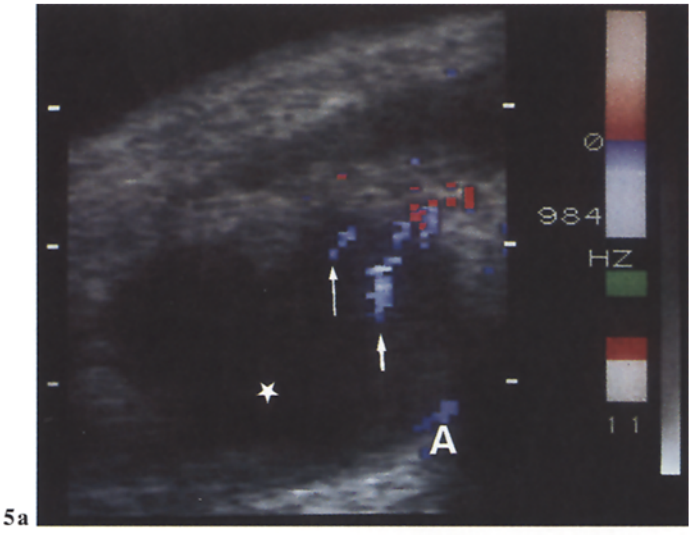

5a

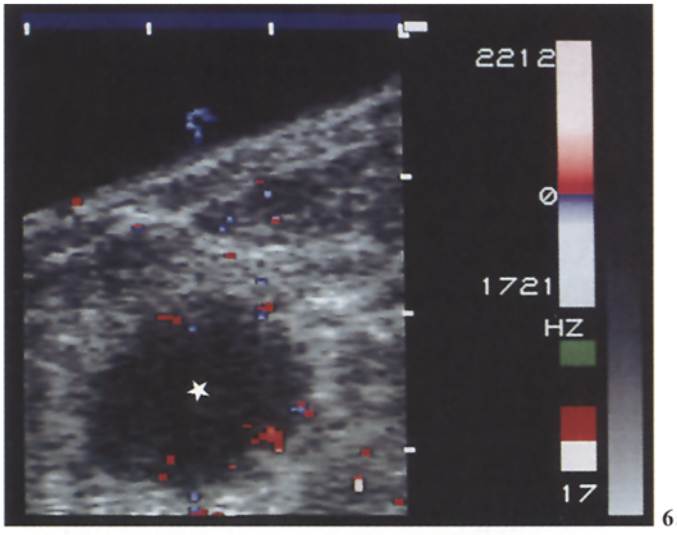

6a

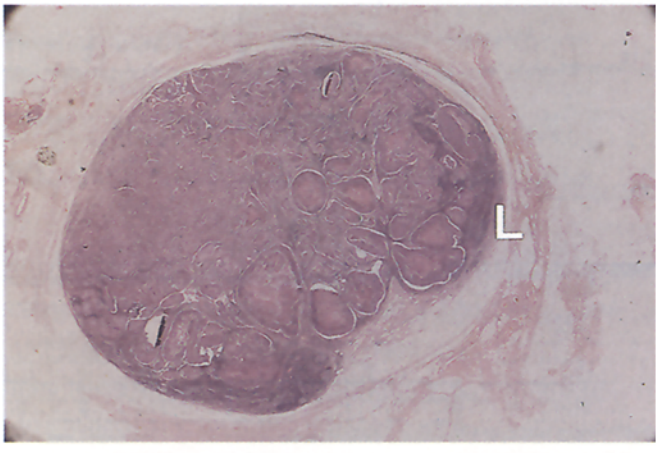

5b

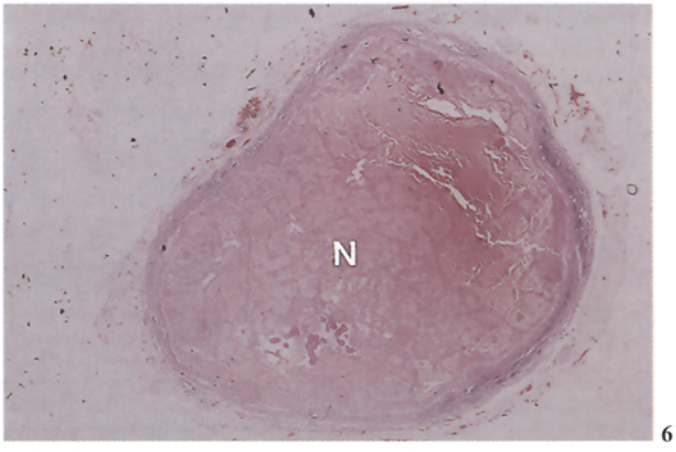

6b

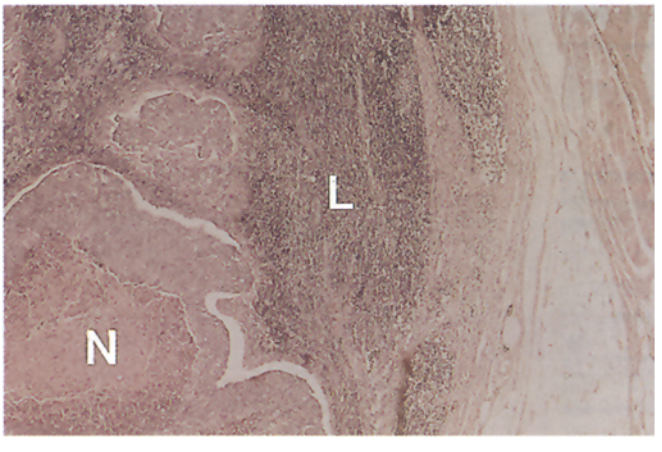

5c

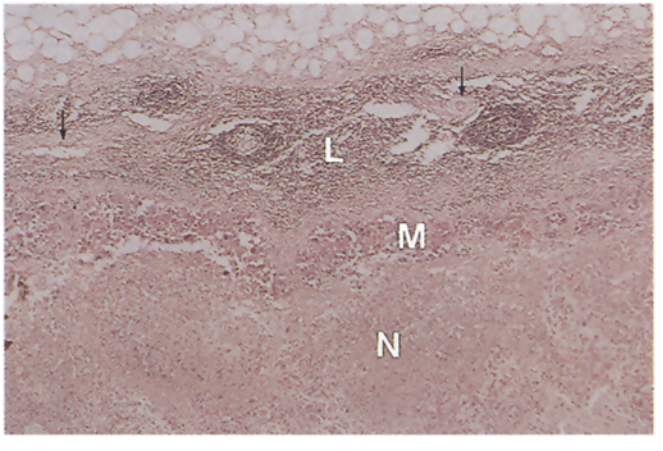

6c

Fig. 5. **a** Cervical lymph node (24 × 18 mm) showing a large avascular area *(asterisk)*, an aberrant central vessel (→), and an accessory peripheral vessel (→). Sonomorphology: round shape, missing echoic center. *A*-adjacent extranodal vessel. **b, c** Histopathology (hematoxylin and eosin staining): lymph node metastasis of a squamous cell carcinoma originating from the pharyngeal tonsil. *N* necrotic areas; *L* residual lymphatic tissue at the poles of the lymph node

Fig. 6. **a** Axillary lymph node (13 × 16 mm) showing multiple accessory peripheral vessels and a central avascular area *(asterisk)*. The hilar vessels cannot be identified. Sonomorphology: round shape, missing echoic center. **b, c** Histopathology : central necrotic *(N)* lymph node metastasis *(M)* of a malignant melanoma. *L* residual subcapsular lymphatic tissue with vessels (→)

major arteries and veins (37 of 47 hilar vessels, 29 of 36 longitudinal vessels) was found. Color Doppler flow imaging detected sole venous major vessels in 12 lymph nodes and sole arterial major vessels in five lymph nodes. Branching of the major vessels was observed in 25 (44 %) reactive lymph nodes. Branches of second ($n = 25$), third ($n = 11$; Fig. 1), and fourth ($n = 1$) order were detected. Five (9 %) hypovascularized reactive lymph nodes showed only short intranodal vessel segments which could not be assigned anatomically. Three (5 %) reactive lymph nodes showed avascular areas ($n = 2$), aberrant central vessels ($n = 2$), displacement

Table 4. Pathological vascular patterns detected by CDFI in 130 lymph nodes. Of neoplastic lymph node alterations, 70 of 73 showed at least one pathological vascular pattern in contrast to 3 of 57 reactive lymph nodes ($p < 0.001$). All false-negative reclassifications were low-grade non-Hodgkin's lymphomas

	N	Aberrant vessels	Displacement	Avascular areas	Accessory vessels
Lymph node metastases	37	15**	21	30	27*
Squamous cell carcinoma	23	9	14	19	17
Breast cancer	4	2	2	2	1
Malignant melanoma	9	4	5	8	8
Cylindroma	1	0	0	1	1
Malignant lymphomas	36	27**	17	24	18*
Low-grade NHL	13	6	3	8	6
High-grade NHL	18	17	9	13	10
Hodgkin's lymphoma	5	4	5	3	2

** $p < 0.01$ * $p < 0.05$

Table 5. Sonomorphology of 130 reactive and malignant lymph nodes

	Reactive ($n = 57$)	Metastasis ($n = 37$)	Malignant lymphoma ($n = 36$)
Length (mm)***			
≤ 10	27	2	4
11–15	17	10	12
16–30	13	25	20
Thickness (mm)***			
≤ 10	53	7	17
11–15	4	13	13
16–30	0	17	6
Width (mm)***			
≤ 10	39	5	10
11–15	14	15	15
16–30	4	17	11
Echoic center***			
Normal	36	2	4
Narrow	10	3	3
Missing	11	32	29
Hypoechoic rim			
Narrow	32	0	1
Wide	8	2	2
Eccentric	6	2	4
Shape***			
Ellipsoid	51	11	20
Round	6	26	16
Sonomorphological index (Table 1)***			
≤ 1	32	1	1
> 1	25	36	35

*** $p < 0.001$

of intranodal vessels ($n = 2$), and/or accessory peripheral vessels ($n = 2$).

In malignant lymph nodes CDFI demonstrated 47 (64 %) hilar and 7 longitudinal vessels. Longitudinal vessels were displaced in three further lymph nodes. Adjacent arteries and veins were found in 34 pairs of hilar vessels and all longitudinal vessels. A total of 70 (96 %) malignant lymph nodes showed at least one (average 2.5) of the four following pathological alterations of the intranodal vascular patterns (Table 4): (a) avascular areas ($n = 54$), (b) aberrant central vessels ($n = 42$), (c) displacement of intranodal vessels ($n = 38$), or accessory peripheral vessels ($n = 45$). Avascular areas and accessory peripheral vessels were seen more frequently in lymph node metastases. Branching of the longitudinal or aberrant central vessels was seen in 19 (26 %) malignant lymph nodes. Color Doppler flow imaging could only depict short intranodal vessel segments in seven hypovascularized malignant lymph nodes. These vessel segments could be identified as accessory peripheral vessels in six lymph nodes in contrast to the findings in reactive lymph nodes.

Table 6. Reclassification of 130 lymph nodes using different sonographic criteria for malignancy

	Sensitivity (%)	Specificity (%)	Accuracy (%)
Maximum diameter > 10 mm	92	47	72
Minimum diameter > 10 mm	67	93	78
Round shape	58	89	72
Missing echoic center	84	81	82
Wide hypoechoic rim	14	75	41
Sonomorphological index > 1	97	56	79
Pourcelot's ratio ≥ 0.9 or	18	95	52
pulsatility index ≥ 1.8	24	95	67
(only lymph node metastasis)			
Pathological vascular pattern	96	95	95

The maximum diameter (Table 5) was lower than 11 mm in 33 lymph nodes, 11–15 mm in 39 lymph nodes, and higher than 15 mm in the rest ($n = 58$). Forty-two (58 %) malignant and 6 (11 %) reactive lymph nodes had a round shape ($p < 0.001$). The hyperechoic central area was missing in 61 (84 %) malignant and 11 (19 %) reactive lymph nodes ($p < 0.001$). Eccentric widening of the hypoechoic rim was found in six reactive and six malignant lymph nodes. The sonomorphological score (Table 1) exceeded 1 in 71 (97 %) malignant and 25 (44 %) reactive lymph nodes ($p < 0.001$).

The nonparametric discriminant analysis of all evaluated parameters proved that the assessment of the intranodal vascular pattern was the best parameter to differentiate benign from malignant lymphadenopathy (accuracy 95 %). The pattern of the intranodal vascularization was the only parameter which attained a high sensitivity as well as a high specificity (Table 6). All remaining parameters optimized either sensitivity or specificity. All three false-positive reclassifications occurred in patients who suffered from venereal diseases. Hypovascularization (short intranodal vessel segments) was the probable cause of one false-negative reclassification in a patient showing recurrent chronic lymphatic leukemia (lymph node involvement was proven by histopathology). One patient suffering from recurrent lymphoma (centrocytic B-cell lymphoma stage IIIb) showed normal vascular patterns in two hypervascularized lymph nodes. Sonomorphological changes were contradictory in these patients (Table 7).

Table 7. Sonomorphology of six lymph nodes, which were reclassified erroneously by evaluation of the intranodal vascular pattern. CLL chronic lymphatic leukemia (recurrence) with histopathologically proven lymph node involvement; NHL recurrent low-grade non-Hodgkin's lymphoma

	False positive	False positive	False positive	False negative	False negative	False negative
Diagnosis	Ulcus molle	Lues	Lues	CLL	NHL	NHL
Maximum diameter > 10 mm	–	+	+	–	+	+
Minimum diameter > 10 mm	–	+	+	–	+	–
Round shape	–	–	–	–	–	–
Missing echoic center	–	–	–	+	–	–
Wide hypoechoic rim	eccentric	eccentric	+	0	eccentric	–
Sonomorphological index > 1	+	+	+	+	+	–
Pourcelot's ratio ≥ 0.9 or pulsatility index ≥ 1.8	–	–	–	–	–	–

Discussion

Changes in the perfusion in enlarged lymph nodes can be depicted by CT and MRI if they lead to alterations in the contrast enhancement in the tissue. In clinical practice intranodal vessels cannot be evaluated by CT and MRI due to their limited spatial resolution and to divergent directions of the scanning plane and of the intranodal vessels. Ultrasonography can only assess size, shape, and echogenicity of superficial lymph nodes [1–6]. Even when an US frequency of 13 MHz was used, no intranodal vessels were described [12]. Acoustic microscopy (frequency 600 MHz), which can be used to observe arterioles [13], is not suitable for in vivo examinations. Color Doppler flow imaging allows the assessment of intranodal vessels in superficial lymph nodes using individually optimized scanning planes. In order to get a virtual image of the 3D pattern of intranodal vascularization, the whole lymph node has to be assessed carefully on two planes. Spatial resolution of CDFI is sufficient to distinguish adjacent extranodal vessels from peripheral intranodal vessels by rotation of the scanning plane in most cases, but when in doubt a vessel has to be regarded as extranodal. If there are only short intranodal vessel segments or singular color spots, Doppler spectral analysis (which was done in all examinations) distinguishes between color artifacts and flow signals. Pulsations originating from adjacent great vessels which cause intranodal color artifacts may reduce the quality of CDFI studies. Of the assessed lymph nodes, 18 % showed such artifacts, but diagnostic accuracy was not impaired in this group. If the power of the irradiated US or the sensitivity for the display of flow signals (threshold) is set too low, a significant loss of signal strength and diagnostic accuracy occurs. The pulse repetition frequency and the cutoff frequency of the high-pass filters have to be decreased to the minimum values in order to detect very low flow velocities. The inclusion criteria used in this study, which are based on clinical experience, should ensure a standardized high sensitivity for flow signals.

In vitro studies [14] proved that CDFI can measure flow in vessels as small as arterioles (diameter 0.1 mm). These small vessels could only be detected if color flow signals were present. Flow which did not induce Doppler frequency shifts of at least 37.5 Hz could not be depicted. Especially tissue perfusion and small peripheral vessels of the cortex could not be evaluated. That is why the color-coded vascular pattern did not represent the vascularization nor the perfusion of a lymph node. In phantom studies peak flow velocities were underestimated by CDFI in an inverse proportion to the diameter of small tubes [14, 15]. This means that blood flow in small vessels is less probable to be detected by CDFI despite a sufficient flow velocity. This effect may lead to disproportionate changes in the flow signals if quantitative changes in the intranodal perfusion alter the flow velocity as well as the vessel diameter.

The medulla of a lymph node contains multiple fluid-filled lymphatic sinuses, which are probably the cause of the higher echogenicity in the center of normal lymph nodes [5, 16]. The lower number of acoustic interfaces in the solid tissue of the cortex causes a lower echogenicity. Lymph nodes are delimited by a capsule of connective tissue which is perforated merely at the hilus by arteries, veins, and efferent lymphatic vessels. Intranodal branches of arteries and veins follow the trabeculas which run centripetally through the lymphatic tissue. The distribution of the flow signals which were detected by CDFI in most reactive lymph nodes is analogous to the known anatomic structures. The angle of $\leq 30°$ between the axis of the longitudinal vessels and the skin surface was defined on the basis of clinical experience in the assessment of superficial lymph nodes using CDFI. The longitudinal vessels are running parallel to the skin surface in most reactive superficial lymph nodes. An angle of $\leq 30°$ to the skin surface was defined on the basis of clinical experience in order to eliminate erroneous classifications due to inaccurate measurements of the angle or due to an unfavorable direction of insonation.

A chaotic intranodal flow pattern found in malignant lymphadenopathy [17] and central vessels found in lymphadenitis [18, 19] were already mentioned in former publications, but the intranodal vascular pattern was not evaluated systematically. Avascular areas and displacement of vessels are known arteriographic signs of malignant tumors. They could be detected by CDFI in malignant lymphadenopathy as well. Displacement of intranodal vessels can only be diagnosed if their course

can be assessed continuously. Sufficient flow signals in a part of the lymph node are the prerequisite for the diagnosis of avascular areas. A decreasing amplitude of Doppler signals is to be expected proportional to the decrease in the intranodal vessel diameters and flow velocities from the hilus to the cortex. The signal loss with increasing depth has to be taken into account additionally. Avascular areas may only be diagnosed if there are areas with disproportionate missing flow signals in both planes. Low vascularization of a whole lymph node, which may result in the detection of sole short vessel segments, intranodal or at the hilus position, is no sign of malignancy. But hypovascularization makes the assessment of the vascular pattern more difficult. This may lead to a diagnostic uncertainty, although only one false-negative reclassification occurred in hypovascularized lymph nodes. In the future, US contrast media will probably simplify the evaluation of the intranodal vascular pattern in lymph nodes which show low vascularization [20].

Missing vascularization is a rare finding in superficial lymph nodes if technical parameters are optimized. This optimization could not be tested retrospectively if there was no documentation of intranodal flow signals on both planes. That is why 19 lymph nodes (9 reactive, 10 malignant) had to be excluded from the current study, although all settings of the US device were in the defined range. This means that all results of this study are based only on lymph nodes showing vascularization in CDFI.

Retrospectively, the histopathological analog of the four vascular patterns suspicious of malignancy was only found in singular cases. Avascular areas represented necrosis or hypovascularized neoplastic invasion of the lymph node (Fig. 5b, c and Fig. 6b, c). Accessory peripheral vessels may be a sign of neovascularization or represent vessels in residual subcapsular lymphatic tissue (Fig. 6b, c). The cause of the aberrant course of central vessels, which was found in malignant lymphadenopathy, is not known. Displaced central vessels were not demonstrated by histopathology.

The assessment of the intranodal vascular pattern was highly specific (95 %) and at least as sensitive as all evaluated sonomorphological criteria. A broad spectrum of malignant lymph node alterations was included in the study in order to judge the diagnostic value for the differentiation of benign and malignant lymphadenopathy. If there is a known neoplasm which is suspected of lymph node involvement, the frequency of the patterns found in the different groups of neoplastic lymph node alterations may increase the diagnostic certainty.

Avascular areas may have been caused by partial lymph node necrosis or intranodal granulomas in three lymph nodes involved by lues or ulcus molle which were reclassified erroneously. Histopathological findings of these lymph nodes were not available. All false-negative reclassifications occurred in recurrent low-grade non-Hodgkin lymphomas. Due to the low number of lymph nodes in this group it can not yet be decided if there is a lower diagnostic value of CDFI in the diagnosis of low-grade non-Hodgkin's lymphomas. The preceding chemotherapy led to no suspicious vascular pattern in these three lymph nodes.

The evaluation of the intranodal echogenicity was the best sonomorphological parameter to differentiate benign from malignant lymphadenopathy. The higher sensitivity which was attained using CDFI may be caused by a previous detection of malignant lymph node invasion leading to vascular alterations without eradicating the echogenic center or by the exclusion of malignant alterations simulating the echogenic hilus sign [16, 21]. On the other hand, lipomatous atrophy of a lymph node, leading to a homogeneous echogenicity without depictable echoic center, may simulate the sonomorphology of malignant lymph node alterations [16], but will not alter the vascular pattern. The classification limits of the diameters of the lymph nodes were chosen arbitrarily from the wide range of limits proposed in the literature (5–15 mm). The decreasing or increasing of these limits optimizes either sensitivity or specificity. The evaluation of the shape of the lymph nodes (accuracy 72 %) did not reach the accuracy (85–95 %) reported in former studies [3, 5], probably because of the more inhomogeneous population of lymph nodes which were included. Doppler spectral analysis proved to be useless for the detection of malignant lymphomas just as in a former study [6]. Being aware of the problem of missing diastolic flow signals in quantitative analysis of Doppler spectra, leading to false-high indices, a lot of care was taken to detect these low-frequency Doppler signals. This may be the cause why we did not reach the same sensitivity (48–53 %) for the detection of metastases as in our former study [6]. Two studies [7, 19] proposed the use of lower limits of the Doppler indices as a sign of metastatic lymph node involvement by head and neck tumors and reached a sensitivity of 76–86 %, but a lower specificity of 71–82 % if all assessed lymph nodes were included. These criteria were not tested in the present study.

Conclusion

Pathological vessels are a known angiographic sign of malignant tumors. Using CDFI the present study defined four patterns of intranodal vascularization which proved to be highly sensitive as well as highly specific for the detection of malignant lymphadenopathy. Using these criteria CDFI allowed to reclassify correctly 95 % of 130 superficial lymph nodes. The current retrospective study was the first one which tried to classify meticulously intranodal vascular patterns. The encouraging results are raising, on the other hand, many questions which have to be answered by ongoing and future prospective studies: the intra- and interobserver variability, a correlation of the vascular patterns with histopathological findings, the limits of the application in small hypovascularized lymph nodes or in the case of small intranodal metastases, the optimum parameter settings, and the use of different color Doppler equipment which show large differences in the detection of low-amplitude and low-frequency Doppler signals and in spatial resolu-

tion. The diagnostic accuracy of the proposed criteria of malignancy using CDFI was higher than that of all tested sonomorphological criteria; nevertheless, observer bias by sonomorphological changes cannot be excluded. The classification of the vascular pattern is a subjective decision which may be altered involuntarily by diagnostic information extracted from the B-mode image especially in hypovascularized lymph nodes. Therefore, definitive interpretation of the data requires confirmation by other authors as well as a prospective evaluation.

References

1. Bruneton JN, Roux P, Caramella E, Demard F, Vallicioni J, Chauvel P (1984) Ear, nose and throat cancer: ultrasound diagnosis of metastasis to cervical lymph nodes. Radiology 152: 771–773
2. Leicher-Düber A, Bleier R, Düber C, Thelen M (1990) Halslymphknotenmetastasen: Histologisch kontrollierter Vergleich von Palpation, Sonographie und Computertomographie. RöFo 153: 575–579
3. Steinkamp HJ, Hosten N, Langer R, Mathe F, Ehritt C, Felix R (1992) Halslymphknotenmetastasen. Sonographischer Malignitätsnachweis. RöFo 156: 135–141
4. Prayer L, Winkelbauer F, Gritzmann N, Weislein H, Helmer M, Pehamberger H (1989) Untersuchung der primären Lymphknotenstationen beim malignen Melanom mittels hochauflösender Real-time-Sonographie – Stellenwert und Indikation. RöFo 151: 294–297
5. Vassallo P, Wernecke K, Roos N, Peters PE (1992) Differentiation of benign from malignant superficial lymphadenopathy: the role of high-resolution US. Radiology 183: 215–220
6. Tschammler A, Gunzer U, Reinhart E, Höhmann D, Feller AC, Müller W, Lackner K (1991) Dignitätsbeurteilung vergrösserter Lymphknoten durch qualitative und semiquantitative Auswertung der Lymphknotenperfusion mit der farbkodierten Duplexsonographie. RöFo 154: 414–418
7. Schreiber J, Mann W, Lieb W (1993) Farbduplexsonographische Messung der Lymphknotenperfusion: Ein Beitrag zur Diagnostik der zervikalen Metastasierung. Laryngorhinootologie 72: 187–192
8. Herman PG, Yamamoto I, Mellins HZ (1972) Blood microcirculation in the lymph node during the primary immune response. J Exp Med 136: 697
9. Herman PG, Lyonnet D, Fingerhut R, Tuttle RN (1976) Regional blood flow to the lymph node during the immune response. Lymphology 9: 101–104
10. Feldmann F, Habif DV, Fleming RJ, Kanter IE, Seaman WB (1967) Arteriography of the breast. Radiology 89: 1053–1061
11. Anacker H, Gaul A, Bernett P (1970) Die Arteriographie des Mammakarzinoms. RöFo 113: 448–456
12. Bruneton JN, Balu-Maestro C, Marcy P-Y, Melia P, Mourou M-Y (1994) Very high frequency (13 MHz) ultrasonographic examination of the normal neck: detection of normal lymph nodes and thyroid nodules. J Ultrasound Med 13: 87–90
13. Neild TO, Attal J, Saurel JM (1985) Images of arterioles in unfixed tissue obtained by acoustic microscopy. J Microscopy 139: 19–25
14. Tschammler A, Vieser G, Schindler R, Schuermann R, Krahe T (1993) Ultrasound contrast medium: in-vitro studies. J Ultrasound Med 12 (Suppl 33, abstract)
15. Tschammler A, Rinneberg A, Schindler R, Landwehr P, Krahe T (1992) Farbduplexsonographie kleiner Gefässe im in-vitro Modell. In: Anderegg A, Despland P, Henner H, Otto R (eds) Ultraschalldiagnostik '91. Springer, Berlin Heidelberg New York pp 121–124
16. Rubaltelli L, Proto E, Salmaso R, Bortoletto P, Candiani F, Cagol P (1990) Sonography of abnormal lymph nodes in vitro: correlation of sonographic and histologic findings. AJR 155: 1241–1244
17. Turlington BS, Reading CC, Charboneau JW (1991) Color Doppler US in the neck: differentiating neoplastic from nonneoplastic lymphadenopathy. Radiology 181 (Suppl 177, abstract)
18. Ohnesorge I, Konig H, Schill S, Wolf KJ (1991) Color-coded duplex sonography of pathological enlarged lymph nodes. Radiology 181 (Suppl 177, abstract)
19. Steinkamp HJ, Rausch M, Mäurer J, Holsten N, Schedel H, Langer R, Felix R (1994) Farbkodierte Duplexsonographie in der Differentialdiagnostik zervikaler Lymphknotenvergrösserungen. RöFo 161: 226–232
20. Tschammler A, Krahe T, Wittenberg G, Jenett M (1993) Contrast enhanced color Doppler flow imaging of superficial lymph nodes and correlation with dynamic MRI. Echocardiography 10: 682 (abstract)
21. Evans RM, Ahuja A, Metreweli C (1993) The linear echogenic hilus in cervical lymphadenopathy – a sign of benignity or malignancy? Clin Radiol 472: 262–264